These observations provide direct evidence of the coupling between Io and the Jovian ionosphere, marking the (localized) impact of Io-accelerated charged particles in Jupiter's ionosphere. Further observations of the IFT foot may provide additional information regarding the interaction of Io and Jupiter's magnetosphere, the source location and generation of DAM, and Jupiter's magnetic field.

REFERENCES AND NOTES

1. B. F. Burke and K. L. Franklin, *J. Geophys. Res.* **60**, 213 (1955).
2. T. D. Carr, M. D. Desch, J. K. Alexander, in *Physics of the Jovian Magnetosphere*, A. Dessler, Ed. (Cambridge Univ. Press, Cambridge, 1983), pp. 1–50.
3. E. K. Bigg, *Nature* **203**, 1008 (1964).
4. J. H. Piddington and J. F. Drake, *ibid.* **217**, 935 (1968).
5. P. Goldreich and D. Lynden-Bell, *Astrophys. J.* **156**, 59 (1969).
6. The general description of this type of interaction, applied to the orbital decay of the Echo satellite, was given by S. D. Drell, H. M. Foley, and M. A. Ruderman [*J. Geophys. Res.* **70**, 3131 (1965)]; extension of this work and application to Io was done by F. M. Neubauer [*ibid.* **85**, 1171 (1980)], C. K. Goertz and P. A. Deift [*Planet. Space Sci.* **21**, 1399 (1973)], and C. K. Goertz [*J. Geophys. Res.* **85**, 2949 (1980)].
7. N. F. Ness *et al.*, *Science* **204**, 982 (1979).
8. M. H. Acuña, F. M. Neubauer, N. F. Ness, *J. Geophys. Res.* **86**, 8513 (1981); D. J. Southwood *et al.*, *ibid.* **85**, 5959 (1980).
9. R. L. Baron *et al.*, *Nature* **353**, 539 (1991); S. J. Kim *et al.*, *ibid.*, p. 536. The H_3^+ ion was first detected spectroscopically by P. Drossart *et al.* [*ibid.* **340**, 539 (1989)].
10. R. L. Baron *et al.*, *ibid.*, in press.
11. J. E. P. Connerney, in *Planetary Radio Emissions III*, H. Rucker, M. L. Kaiser, S. J. Bauer, Eds. (Austrian Academy of Sciences Press, Vienna, 1992), pp. 13–33; ———, M. H. Acuña, N. F. Ness, in preparation.
12. Y. H. Kim, J. Fox, H. S. Porter, *J. Geophys. Res.* **97**, 6093 (1992).
13. F. M. Neubauer, *ibid.* **85**, 1171 (1980).
14. D. A. Gurnett and C. K. Goertz, *ibid.* **86**, 717 (1981); Y. Leblanc and F. Bagenal, in *Planetary Radio Emissions II*, H. O. Rucker, S. J. Bauer, B. M. Pedersen, Eds. (University of Graz, Graz, Austria, 1988), pp. 127–138.
15. For a review of potential generation mechanisms for DAM, see M. L. Goldstein and C. K. Goertz, in (*2*), pp. 317–352.
16. A. L. Broadfoot *et al.*, *J. Geophys. Res.* **86**, 8259 (1981).
17. J. Caldwell, B. Turgeon, X.-M. Hua, *Science* **257**, 1512 (1992); V. Dols, J. C. Gérard, F. Paresce, R. Prangé, A. Vidal-Madjar, *Geophys. Res. Lett.* **19**, 1803 (1992); J. C. Gérard, V. Dols, F. Paresce, R. Prangé, *J. Geophys. Res.*, in press.
18. T. A. Livengood *et al.*, *Icarus* **97**, 26 (1992).
19. All mosaics were constructed by cross-correlation of the reduced (sky-subtracted, flattened, less bad pixels) 3.40-μm images, each of which was acquired with an effective integration time of 30 s and ~1% spectral resolution. Image smear attributable to Jupiter's rotation is negligible (Jupiter rotates by only 0.3° in longitude during each exposure). A full mosaic requires ~13 min of observation, during which Jupiter rotates by 8° longitude. Each mosaic is labeled with the central meridian longitude (CML) (in System III) of the center image, which may differ from that of the first or last image by no more than 4°. Limb fitting was accomplished by cross correlation with a limb-brightened model planet, excluding the bright polar region. A red leak correction was made with the use of a similar set of images at 4.9 μm acquired contemporaneously. Each pixel subtends 0.35 arc sec; tracking and positional errors introduced in construction of the mosaic are estimated to be subpixel in magnitude. Image times are Hawaii Standard Time (HST), related to Universal Time (UT) by UT = HST + 10 hours.
20. J. E. P. Connerney, M. H. Acuña, N. F. Ness, *J. Geophys. Res.* **86**, 8370 (1981).

21. We acknowledge the assistance of IRTF telescope operators D. Griep, C. Kaminski, and W. Golish and thank R. Joseph and the staff of the Institute for Astronomy at the University of Hawaii at Manoa. We acknowledge the assistance of J. Harrington, who was instrumental in the acquisition and processing of many of these images, and discussions with colleagues S. Miller, M. J. Mumma, T. J. Birmingham, and T. A. Livengood. Supported by the Yamada Science Foundation, Japan (T.S.). J.E.P.C. is a visiting astronomer at IRTF, which is operated by the University of Hawaii under contract to NASA.

8 June 1993; accepted 13 September 1993

Dependence of Calmodulin Localization in the Retina on the NINAC Unconventional Myosin

Jeffery A. Porter, Mujun Yu, Stephen K. Doberstein, Thomas D. Pollard, Craig Montell

Calmodulin is a highly conserved regulatory protein found in all eukaryotic organisms which mediates a variety of calcium ion–dependent signaling pathways. In the *Drosophila* retina, calmodulin was concentrated in the photoreceptor cell microvillar structure, the rhabdomere, and was found in lower amounts in the sub-rhabdomeral cytoplasm. This calmodulin localization was dependent on the NINAC (neither inactivation nor afterpotential C) unconventional myosins. Mutant flies lacking the rhabdomere-specific p174 NINAC protein did not concentrate calmodulin in the rhabdomere, whereas flies lacking the sub-rhabdomeral p132 isoform had no detectable cytoplasmic calmodulin. Furthermore, a defect in vision resulted when calmodulin was not concentrated in the rhabdomeres, suggesting a role for calmodulin in the regulation of fly phototransduction. A general function of unconventional myosins may be to control the subcellular distribution of calmodulin.

The intracellular Ca^{2+} receptor calmodulin is a primary mediator of Ca^{2+}-dependent signaling in most eukaryotic cells (*1*). It is among the most highly conserved proteins, differing between vertebrates and *Drosophila* in only 3 of 148 amino acids (*2*). Upon binding Ca^{2+}, calmodulin undergoes a conformational change rendering the protein competent to bind and alter the activities of target proteins (*1*). Thus, many proteins including protein kinases, protein phosphatases, ion channels, Ca^{2+} pumps, nitric oxide synthetase, inositol triphosphate kinase, and cyclic nucleotide phosphodiesterase are regulated by intracellular Ca^{2+} concentrations by calmodulin (*1*).

The Ca^{2+} ion plays a central role in light adaptation in vertebrate vision and may be involved in both adaptation and excitation in invertebrate phototransduction. Calmodulin could be one of the primary mediators of the Ca^{2+} response in phototransduction (*3*). Vertebrate rod photoreceptor cells contain calmodulin, which might have a direct role in modulating ion channels gated by guanosine 3′,5′-monophosphate (cGMP) (*4*). Ion channels required for invertebrate phototransduction may also be regulated by calmodulin. Calmodulin is present in the invertebrate microvillar rhabdomeres of photoreceptor cells in the crayfish, squid, and blowfly (*5*). Furthermore, *Drosophila* has a retinal-specific calmodulin binding protein, TRP-L, which has sequence similarity to the photoreceptor-specific putative Ca^{2+} channel, TRP (*6–8*).

The rhabdomere, the specialized microvillar structure of the invertebrate photoreceptor, contains rhodopsin and other important components in phototransduction and is functionally analogous to the outer segments of vertebrate rod cells, which contain calmodulin. In addition, the microvillar rhabdomeres are structurally similar to the calmodulin-rich brush border of vertebrate intestinal epithelial cells (*9*). Like the brush borders, rhabdomeres consist of highly ordered microvilli composed of actin filaments connected to the surrounding plasma membrane by radial links (*9*).

The major calmodulin binding protein in the intestinal microvilli is an unconventional myosin called the brush border myosin I (*10*). Abundant unconventional myosins, NINAC (neither inactivation nor afterpotential C) p132 and p174, are found in *Drosophila* photoreceptor cells and consist of a protein kinase domain joined to a region homologous to the myosin heavy

J. A. Porter, M. Yu, C. Montell, Departments of Biological Chemistry and Neuroscience, The Johns Hopkins University School of Medicine, Baltimore, MD 21205. S. K. Doberstein and T. D. Pollard, Department of Cell Biology and Anatomy, The Johns Hopkins University School of Medicine, Baltimore, MD 21205.

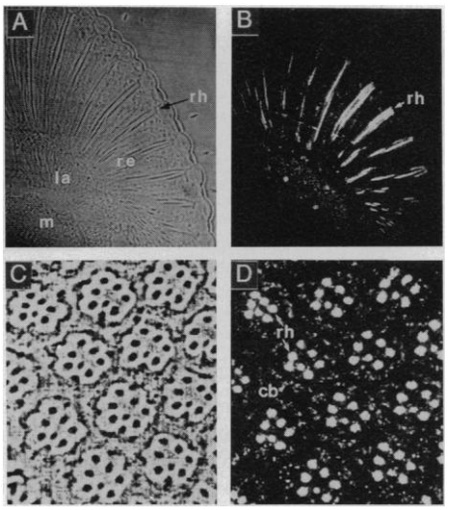

Fig. 1. Spatial distribution of calmodulin in the adult *Drosophila* compound eye. The images in (**A**) and (**B**) are phase contrast and immunofluorescence images of a 0.5-μm longitudinal plastic section of an adult eye. Calmodulin was detected by indirect immunofluorescence staining with a rabbit antibody to calmodulin used as the primary antiserum and a goat fluorescein-labeled secondary antibody to rabbit. Tissue sections were prepared and processed as described (*20*). The specificity of the calmodulin antiserum is shown in Fig. 3. Indicated are the lamina (la), medulla (m), retina (re), and rhabdomeres (rh). The images in (**C**) and (**D**) are phase contrast and immunofluorescence images of cross sections of the compound eye stained with an antibody to calmodulin and a fluorescein-labeled secondary antibody. The *Drosophila* compound eye consists of 800 repeat units referred to as ommatidia. Each ommatidium contains 20 cells including eight photoreceptor cells. Six of the eight photoreceptor cells extend the full depth of the ommatidia and two occupy either the upper or lower portions of the ommatidia. Consequently only seven photoreceptor cells are present in any given cross section. Two rhabdomeres and a sub-rhabdomeral cell body (cb) are indicated in (D).

chain head (*11*, *12*). The p174 isoform is spatially restricted to the microvillar rhabdomeres, and p132 is restricted to the subrhabdomeral cytoplasm (*13*). Most unconventional myosins bind calmodulin, although the function of this interaction in vivo has not been clarified (*14*). We report here that interaction between the NINAC unconventional myosin and calmodulin is required for subcellular localization of calmodulin and for phototransduction.

In *Drosophila* photoreceptor cells, calmodulin was highly concentrated in the rhabdomeres (Fig. 1). The rhabdomeres appeared as ribbons of staining extending the length of the retina in longitudinal sections (Fig. 1, A and B) and as seven ovals in each ommatidium in cross sections (Fig. 1, C and D). The sub-rhabdomeral cytoplasm of the photoreceptor cells also stained with antibody to calmodulin (Fig. 1D). We estimate that the concentration of calmodulin in the rhabdomeres was approximately 0.5 mM (*15*).

Two methods were used to examine whether the NINAC proteins bind calmodulin. In the first method, the calmodulin-overlay technique, p174 but not p132 bound calmodulin. Retinal proteins from wild-type and *ninaC* null flies, *ninaC*^{P235}, were fractionated on a polyacrylamide gel, transferred to nitrocellulose, allowed partially to renature, and probed with ^{125}I-calmodulin. The major band detected in this analysis appeared to be NINAC p174 because it was a protein of approximately 170 kD present in the lane containing wild-type extracts and not in the *ninaC*^{P235} lane (Fig. 2A). In a second assay with calmodulin-agarose affinity resin and whole head extracts, we found that both NINAC isoforms bound calmodulin. The proteins from crude high-speed supernatants that bound to calmodulin-agarose were eluted with SDS sample buffer, fractionated on a polyacrylamide gel, and visualized by staining with Coomassie blue. Two polypeptides the sizes of the NINAC proteins were the major calmodulin binding proteins identified in this assay (Fig. 2B). Both of these bands reacted with a *ninaC* antibody, and neither was detected in the calmodulin-agarose assay with *ninaC*^{P235} extracts. The NINAC p174 and p132 isoforms bound calmodulin-agarose in the presence or absence of Ca^{2+}; however, p132 required Ca^{2+} for optimal binding (*16*).

Because the NINAC proteins were the major calmodulin binding proteins in the retina and are putative motor molecules that might play a role in transporting other proteins in photoreceptor cells, we compared the spatial localization of calmodulin in wild-type and several *ninaC* mutants. In *P*[*ninaC*$^{\Delta 132}$] flies, which express p174 but not p132 (*13*), calmodulin was expressed in amounts similar to those in wild-type flies (Fig. 3). It was concentrated in the rhabdomeres, but very little was detected in the sub-rhabdomeral cytoplasm (Fig. 4A). In *P*[*ninaC*$^{\Delta 174}$] flies expressing p132 but not p174 (*13*), calmodulin was expressed at two-thirds the wild-type amount (Fig. 3) and appeared evenly dispersed throughout the cell without strong rhabdomere staining (Fig. 4B).

When both p174 and p132 were absent from the photoreceptors, as in *ninaC*^{P235} flies, the amount of retinal calmodulin was half that of wild-type flies and was localized to the extracellular central matrix (Figs. 3 and 4C). This mislocalization was specific to calmodulin because the subcellular distribution of another rhabdomeric protein, rhodopsin (Rh1), was unchanged in *ninaC*^{P235} (*16*). The localization of calmodulin to the central matrix was unlikely due to retinal degeneration because the localization was assayed in young flies that had undergone little degeneration. Furthermore, in young *retinal degeneration*C (*rdg*C) mutant flies that have undergone a similar degree of subtle retinal degeneration to that in young *ninaC* flies (*17*), calmodulin localization was indistinguishable from that of

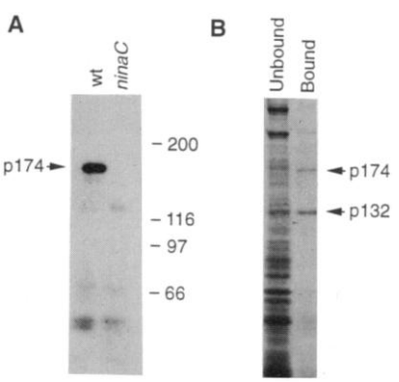

Fig. 2. The NINAC proteins are the major calmodulin binding proteins in the fly retina. (**A**) Identification of retinal calmodulin binding proteins by the calmodulin-overlay technique (*32*). Retinal extracts from wild-type (wt) and *ninaC*^{P235} (*ninaC*) flies were fractionated on an SDS-PAGE (6% gel), transferred to nitrocellulose, and probed with ^{125}I-labeled calmodulin in the presence of 0.1 mM $CaCl_2$. The NINAC p174 protein and position of several protein size markers are indicated. (**B**) Proteins from wild-type fly heads that bound calmodulin-agarose (*33*). Proteins from a high-speed supernatant, prepared from wild-type fly heads, were incubated in batch with calmodulin-agarose in the presence of 1 mM EGTA and washed in buffer containing 1 mM EGTA, and the bound proteins were eluted with 2 × SDS sample buffer (*33*). Proteins remaining in the supernatant (Unbound) and proteins that eluted from the calmodulin-agarose with 2 × SDS sample buffer (Bound) were fractionated on an SDS-PAGE (6% gel) and visualized by staining with Coomassie blue. The two NINAC proteins, p132 and p174, are indicated.

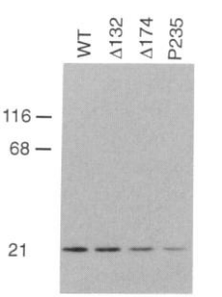

Fig. 3. The amount of calmodulin in the retinas of wild-type and *ninaC* mutant flies. Retinas from wild-type and *P*[*ninaC*$^{\Delta 132}$], *P*[*ninaC*$^{\Delta 174}$], and *ninaC*^{P235} were dissected, fractionated by SDS-PAGE (14% gel), transferred to a polyvinylidene difluoride (PVDF) membrane, and probed with an antibody to calmodulin and subsequently with ^{125}I-labeled protein A (*34*). The positions of protein size standards are indicated. The relative concentrations of calmodulin in each lane were quantified with a PhosphorImage Analyzer (Molecular Dynamics) and storage phosphorscreen.

wild-type flies (Fig. 4D). When calmodulin was not bound to NINAC and properly localized, it might have accumulated in the central matrix during the normal turnover of the photoreceptor cell membrane and contents, which involves the shedding of the microvillar tips (*18*).

We determined the phenotypic consequences of disrupting p174 calmodulin binding by mapping and mutating the calmodulin binding site. This analysis focused on p174 because it is the only NINAC isoform required for wild-type electrophysiology and morphology (*13*). The calmodulin binding domain in p174 was mapped by two independent approaches. The first approach entailed generating random fragments [300 to 800 base pairs (bp)] of the full-length NINAC complementary DNA (cDNA), encoding the 1501 amino acid p174 protein, and subcloning the random fragments into a bacteriophage λ expression library. The expression library was then screened with ^{125}I-calmodulin, and 19 positives were identified. Each of the *ninaC* cDNA inserts was then amplified by the polymerase chain reaction (PCR), and the DNA sequences of the two ends were determined. All 19 positives mapped to the same region of the cDNA encoding the myosin head-tail junction (*19*) (Fig. 5A).

The second method entailed calmodulin overlays and calmodulin-agarose assays with mutant p174 polypeptides expressed in transgenic flies. These included P[*ninaC*^{KD}] and P[*ninaC*^{MD}] flies, which express stable forms of p174 missing the kinase and myosin domains, respectively (Fig. 5C) (*20, 21*). In addition, we generated another transformant line, P[*ninaC*$^{\Delta B}$], which expressed a stable derivative of p174 missing the NH_2-terminal region of the p174 tail extending from amino acids 1037 to 1253 (*21*) (Fig. 5A). The mutation in P[*ninaC*$^{\Delta B}$] flies, in addition to truncating p174, prevented synthesis of p132.

The deletion of 217 amino acids beginning at the end of the myosin head region in p174 eliminated all detectable calmodulin binding on calmodulin overlays; however, the deletion of the myosin or kinase domains did not affect association with calmodulin (Fig. 5B). Similar results were obtained in solution by the binding of extracts, prepared from heads of wild-type flies, to calmodulin-agarose and probing for the NINAC proteins on a protein immunoblot (Fig. 5C). In wild type, P[*ninaC*^{KD}], and P[*ninaC*^{MD}], the various derivatives of p174 bound to calmodulin, whereas the truncated large NINAC protein from P[*ninaC*$^{\Delta B}$] did not (Fig. 5C). The two assays demonstrated that the region from residues 1037 to 1253 was the only domain in p174 required for calmodulin binding in vitro. This domain contains two sequences

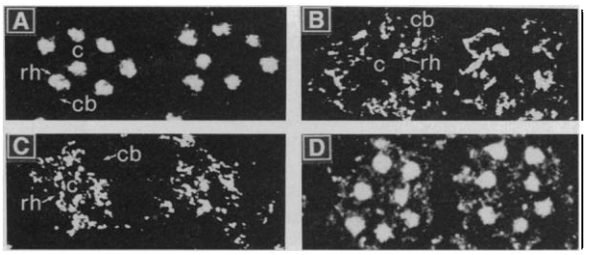

Fig. 4. Subcellular localization of calmodulin in *ninaC* mutant compound eyes. Indirect immunofluorescence staining of calmodulin on 0.5-μm plastic cross sections of compound eyes (*35*): (**A**) P[*ninaC*$^{\Delta 132}$], (**B**) P[*ninaC*$^{\Delta 174}$], (**C**) *ninaC*^{P235}, and (**D**) *rdgC*. Several photoreceptor cell rhabdomeres and cell bodies as well as the central matrix (c) in the extracellular space of several ommatidia are indicated.

of approximately 25 amino acids, referred to as IQ motifs, found in the calmodulin binding region of other unconventional myosins and the neuron-specific calmodulin binding protein neuromodulin (GAP-43) (*14, 22*).

Examination of the spatial localization of calmodulin in P[*ninaC*$^{\Delta B}$] compound eyes provided in vivo evidence that the NH_2-terminal region of the p174 tail is the calmodulin binding domain. The 145-kD truncated derivative of p174, expressed in P[*ninaC*$^{\Delta B}$], was restricted to the rhabdomeres just as in wild-type flies (Fig. 6, A and B), but most of the calmodulin in P[*ninaC*$^{\Delta B}$] ommatidia was in the extracellular central matrix rather than in the rhabdomeres and sub-rhabdomeral cytoplasm (Fig. 6, C and D). The levels of calmodulin in P[*ninaC*$^{\Delta B}$] retinas were reduced approximately twofold, as was observed with *ninaC*^{P235} (Fig. 6E).

We used electroretinogram (ERG) recordings, which measure the responses of retinal cells to light, to determine whether there was a defect in phototransduction associated with P[*ninaC*$^{\Delta B}$] flies. In wild-type flies, there was a large corneal negative response to light followed by a rapid return to the dark state upon the cessation of the light stimulus (Fig. 7). The large transient spike coincident with termination of the light pulse, the off-transient, derives from activity in the laminal portion of the optic lobe (*23*). The response of wild-type flies to a second pulse of light was indistinguishable from the first (Fig. 7).

The P[*ninaC*$^{\Delta B}$] flies showed an ERG phenotype characteristic of the null allele, *ninaC*^{P235}. The features of this defective ERG included an abnormally large initial response, a significantly reduced off-transient, and a slow return to base line upon the cessation of the first light pulse (Fig. 7). These results indicated that deletion of the calmodulin binding domain in p174 caused a defect in phototransduction.

The P[*ninaC*$^{\Delta B}$] flies did not undergo the

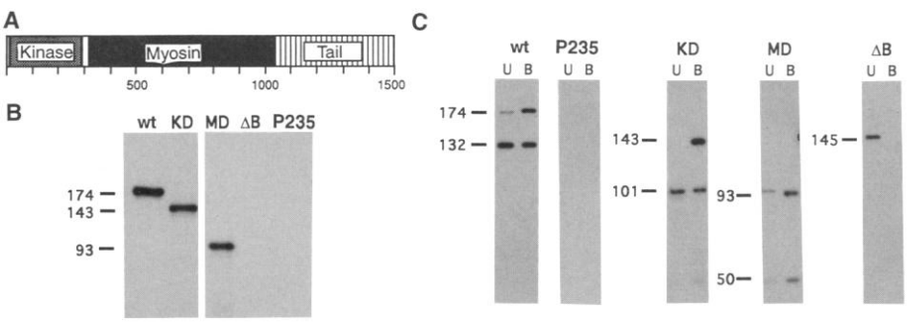

Fig. 5. Mapping of the p174 calmodulin binding domain to the myosin head tail junction. (**A**) Domain structure of p174. The protein kinase and myosin head and tail domains are represented by the stippled, black, and striped boxes, respectively. The diagram of p174 is demarcated in amino acids (shown below). (**B**) Mapping of the calmodulin binding domain by the calmodulin-overlay technique. Retinal extracts from wild type, P[*ninaC*^{KD}] (KD), P[*ninaC*^{MD}] (MD), P[*ninaC*$^{\Delta B}$] (ΔB), and *ninaC*^{P235} (P235) were fractionated by SDS-PAGE (6% gel), transferred to nitrocellulose, and probed with ^{125}I-calmodulin in the presence of 0.1 mM $CaCl_2$ (*21, 32*). The sizes of the wild-type p174 protein and the deleted forms in P[*ninaC*^{KD}] and P[*ninaC*^{MD}] are indicated in kilodaltons. (**C**) Binding of truncated derivatives of p174 to calmodulin-agarose. Proteins from a high-speed supernatant, prepared from wild-type and mutant fly heads, were incubated in batch with calmodulin-agarose in the presence of 1 mM $CaCl_2$ (*33*). The calmodulin-agarose was then washed in buffer containing 1 mM $CaCl_2$, and the bound proteins were eluted with 2 × SDS sample buffer (*33*). Unbound proteins remaining in the supernatant (U) and proteins that bound and were eluted from the calmodulin-agarose with 2 × SDS sample buffer (B) were fractionated by SDS-PAGE (6% gel) and transferred to nitrocellulose. The NINAC proteins were visualized by probing with rabbit antisera specific to the p132 and p174 tails (α132 and α174) and with ^{125}I–protein A as described (*13*). The sizes of the wild-type and truncated derivatives of p174 and p132 are indicated in kilodaltons.

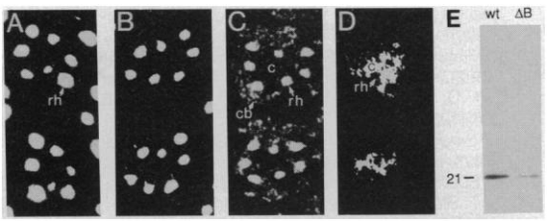

Fig. 6. The *P*[*ninaC*$^{\Delta B}$] flies show aberrant calmodulin distribution and a reduction in calmodulin protein levels. (**A** and **B**) Indirect immunofluorescence staining of cross sections of wild-type and *P*[*ninaC*$^{\Delta B}$] compound eyes, respectively, with a NINAC p174–specific antibody (*13*). A rhabdomere is indicated (rh). (**C** and **D**) Indirect immunofluorescence staining of cross sections of wild-type and *P*[*ninaC*$^{\Delta B}$] compound eyes, respectively, with a calmodulin-specific antibody. The extracellular central matrix, a rhabdomere, and a sub-rhabdomeral cell body are indicated in (C). (**E**) Protein immunoblot of retinal proteins from wild-type and *P*[*ninaC*$^{\Delta B}$] (ΔB) flies probed with a calmodulin antibody.

age- and light-dependent retinal degeneration that characterizes *ninaC*^{P235} (*13*). Thus, the disruption of the NINAC-calmodulin interaction and consequent mislocalization of calmodulin did not cause retinal degeneration. These results also demonstrated that a *nina*C null ERG phenotype can be obtained without causing retinal degeneration. Although it is possible that the NINAC deletion in *P*[*ninaC*$^{\Delta B}$] flies may affect some function in addition to calmodulin binding, the deletion does not alter the subcellular distribution of p174 or affect the ability of NINAC to maintain the rhabdomeres.

Calmodulin localized in the vertebrate rod outer segment may modulate phototransduction because calmodulin affects the affinity of cGMP-gated ion channels for cGMP in vitro (*4*). The high concentration of calmodulin in the rhabdomeres is consistent with a role for calmodulin in mediating the Ca^{2+} signals that are central to the invertebrate photoresponse. The invertebrate phototransduction cascade uses Ca^{2+} as the principal messenger for light adaptation, a feature shared with vertebrate vision (*3*). The Ca^{2+} ion has also been implicated in the excitation step, partly on the basis of the phenotype of the phospholipase C–deficient mutant *norpA* (*24*) and electrophysiological analyses of *trp* mutant flies that are missing a light-activated Ca^{2+} current (*8*).

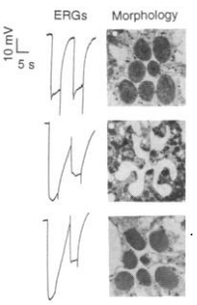

Fig. 7. Electrophysiological and morphological phenotype of *P*[*ninaC*$^{\Delta B}$] flies. (**Top**) Wild-type, (**Middle**) *ninaC*^{P235}, and (**Bottom**) *P*[*ninaC*$^{\Delta B}$] flies were analyzed by ERG recordings as described in (*13*). Briefly, the flies were dark-adapted for 60 s before being exposed to two 4-s pulses of bright light separated by a 5-s dark adaption. The on-transient was typically reduced or absent in these ERGs because of limitations in the sampling rate of the MacLab analog-digital converter (Division of ADI instruments, Milford, Massachusetts). The morphology of wild-type, *ninaC*^{P235}, and *P*[*ninaC*$^{\Delta B}$] ommatidia was assessed by transmission electron microscopic examination of cross sections of compound eyes at a depth of 30 μm. Retinal degeneration was assessed after the flies were maintained for 21 days on a 12-hour light–12-hour dark cycle.

Calmodulin has several potential roles in *Drosophila* vision because it activates the in vitro activities of various protein kinases, channels, cyclases, and phosphodiesterases in other signaling systems. Calmodulin may modulate ion channel activity in the fly eye as it appears to in vertebrates. In addition, calmodulin might regulate adenylyl cyclase in the retina because type I calmodulin–sensitive adenylyl cyclase is expressed in the vertebrate retina (*25*). One potential role for rhabdomeric calmodulin is to regulate p174 function. Alternatively, the calmodulin could translocate from p174 to other rhabdomeric proteins as part of a mechanism to regulate their activities. Calmodulin could also make up a Ca^{2+} buffering system within the rhabdomere.

Because neuronal degeneration is associated with defective Ca^{2+} homeostasis, it has been suggested that Ca^{2+} binding proteins, such as calmodulin, may prevent degeneration in certain neuronal cells (*26*). However, the decrease in rhabdomeral calmodulin concentration in the *nina*C mutant *P*[*ninaC*$^{\Delta B}$] did not lead to the degeneration of the photoreceptors. Therefore, either there was not a large increase in free Ca^{2+} levels in *P*[*ninaC*$^{\Delta B}$] rhabdomeres or an increase in free Ca^{2+} does not cause degeneration in photoreceptor cells. Previous mutational analyses have suggested that the p174 protein has multiple functions in photoreceptor cells (*20*). One of these roles could be to control the subcellular localization of calmodulin in the photoreceptor cells.

In addition to NINAC, other proteins may transport calmodulin, retain it, or both in various subcellular locations. The neuron-specific calmodulin binding protein neuromodulin (GAP-43) has been proposed to localize calmodulin at specific sites within neurons (*27*). Brush border myosin I, the major calmodulin binding protein of the brush border, is localized to the microvilli of intestinal epithelial cells where the calmodulin concentration is approximately 0.6 mM (*10*, *28*). The *Saccharomyces cerevisiae* unconventional myosin MYO2 is required for bud site formation and subsequent cell division (*29*). Calmodulin localizes almost exclusively to the bud site in normal dividing yeast cells but fails to localize in actin mutants (*30*). These results suggest that the proper distribution of yeast calmodulin may require interaction with MYO2 (*30*). A putative unconventional myosin in *Dictyostelium* has been shown to localize to the contractile vacuole, a site where high concentrations of calmodulin are found (*31*). Thus, control of the subcellular localization of calmodulin may be a general function of many unconventional myosins.

REFERENCES AND NOTES

1. C. B. Klee, *Biochemistry* **16**, 1017 (1977); J. R. Dedman *et al.*, *J. Biol. Chem.* **252**, 8415 (1977); D. J. Wolff, P. G. Poirer, C. O. Brostrom, M. A. Brostrom, *ibid.*, p. 4108; K. B. Seamon, *Biochemistry* **19**, 207 (1980); C. B. Klee and T. C. Vanaman, *Adv. Protein Chem.* **35**, 213 (1982); K. K. Wang *et al.*, *Biochem. J.* **262**, 693 (1989); D. S. Bredt and S. H. Snyder, *Proc. Natl. Acad. Sci. U.S.A.* **87**, 682 (1990).
2. V. L. Smith *et al.*, *J. Mol. Biol.* **196**, 471 (1987); M. K. Yamanaka *et al.*, *Nucleic Acids Res.* **15**, 3335 (1987).
3. K. W. Koch and L. Stryer, *Nature* **334**, 64 (1988); A. M. Dizhoor *et al.*, *Science* **251**, 915 (1991); H. G. Lambrecht and K. W. Koch, *EMBO J.* **10**, 793 (1991); B. Minke and Z. Selinger, in *Neuromethods*, A. Boulton, G. Baker, C. Taylor, Eds. (Humana Press, Totowa, NJ, 1992), p. 517; D. P. Smith *et al.*, *Annu. Rev. Cell Biol.* **7**, 161 (1991); K. Nagy, *Q. Rev. Biophys.* **24**, 165 (1991).
4. R. E. Kohnken *et al.*, *J. Biol. Chem.* **256**, 12517 (1981); S. Nagao, A. Yamazaki, M. W. Bitensky, *Biochemistry* **26**, 1659 (1987); Y. T. Hsu and R. S. Molday, *Nature* **361**, 76 (1993).
5. H. G. de Couet, P. P. Jablonski, J. L. Perkin, *Cell Tissue Res.* **244**, 315 (1989).
6. C. Montell and G. M. Rubin, *Neuron* **2**, 1313 (1989); F. Wong *et al.*, *ibid.* **3**, 81 (1989).
7. A. M. Phillips *et al.*, *ibid.* **8**, 631 (1992).
8. R. C. Hardie and B. Minke, *ibid.*, p. 643.
9. M. S. Mooseker, *Annu. Rev. Cell Biol.* **1**, 209 (1985); K. Arikawa, J. L. Hicks, D. S. Williams, *J. Cell Biol.* **110**, 1993 (1990).
10. J. R. Glenney and K. Weber, *J. Biol. Chem.* **255**, 551 (1980); J. H. Collins and C. W. Borysenko, *ibid.* **259**, 14128 (1984).
11. C. Montell and G. M. Rubin, *Cell* **52**, 757 (1988).
12. H. Matsumoto, K. Isono, Q. Pye, W. L. Pak, *Proc. Natl. Acad. Sci. U.S.A.* **84**, 985 (1987).
13. J. A. Porter, J. L. Hicks, D. S. Williams, C. Montell, *J. Cell Biol.* **116**, 683 (1992).
14. R. E. Cheney and M. S. Mooseker, *Curr. Opin. Cell Biol.* **4**, 27 (1992). The IQ motif has been suggested as being important to calmodulin binding. NINAC p174 has two IQ motifs, one of which is common to p132 and p174 (the Q is at amino acid 1044) and a second that is unique to p174 (the Q is at amino acid 1080).
15. To estimate the calmodulin concentration in wild-type rhabdomeres, we dissected 25 fly retinas from flies collected <24 hours posteclosion and dehydrated the retinas overnight in acetone at −20°C as described by H. Matsumoto, J. E. O'Tousa, and W. L. Pak [*Science* **217**, 839 (1982)]. The retinas were homogenized in a 1.5-ml microfuge tube, with a microfuge tube pestle (Kontes Biotechnology, Vineland, NJ), in 25 μl of 2× SDS sample buffer. Samples (12 μl) of each homogenate were fractionated by SDS–polyacryl-

amide gel electrophoresis (PAGE) (14% gel) along with bovine calmodulin as a standard for the estimation of the retinal calmodulin concentration on a Coomassie blue stained gel. *Drosophila* calmodulin was identified in the gel on the basis of the characteristic change in mobility in the presence of EGTA (~20 kD) or Ca^{2+} (17 kD) [C. B. Klee, T. H. Crouch, M. H. Krinks, *Proc. Natl. Acad. Sci. U.S.A.* **76**, 6270 (1979)]. In addition, the calmodulin was the only major 20-kD retinal protein. Assuming all the retinal calmodulin was in the photoreceptor cells and that >80% of this calmodulin was in the rhabdomeres, we estimated the concentration of calmodulin per rhabdomere at 0.5 pg. Using previously determined measurements of the length and diameter of the *Drosophila* rhabdomere from R. C. Hardie [in *Progress in Sensory Physiology 5*, H. Autrum *et al.*, Eds. (Springer-Verlag, New York, 1983), p. 1] and assuming that 50% of the rhabdomeric volume was cytoplasmic, we estimated that the cytoplasmic volume of a rhabdomere was 0.05 pl and that the concentration of calmodulin in a rhabdomere was 0.5 mmol.

16. J. A. Porter and C. Montell, unpublished material.
17. F. Steele and J. E. O'Tousa, *Neuron* **4**, 883 (1990); F. R. Steele, T. Washburn, R. Rieger, J. E. O'Tousa, *Cell* **69**, 669 (1992).
18. A. D. Blest, in *Advances in Insect Physiology*, P. D. Evans and V. B. Wigglesworth, Eds. (Academic Press, London, 1988), p. 1.
19. The NINAC expression library was constructed by the generation of random size-selected DNA fragments (0.3 to 0.8 kb) from the cDNA, pc-*ninaC*-15 (*11*), encoding the full-length p174 as described by C. Montell, K. Jones, C. Zuker, and G. Rubin [*J. Neurosci.* **7**, 1558 (1987)] and subcloned into the Eco RI site of λgt11 [R. Young and R. Davis, *Proc. Natl. Acad. Sci. U.S.A.* **80**, 1194 (1983); R. A. Young and R. W. Davis, *Science* **222**, 778 (1983)]. The NINAC fragment library was screened with ^{125}I-calmodulin (NEN, Boston) by the method of Phillips and co-workers (*7*), and 19 positives were plague-purified. The *ninaC* DNA inserted between the λ arms was amplified by asymmetric PCR, and the sequences of the ends of each clone were determined by dideoxy sequencing [P. C. McCabe, in *PCR Protocols: A Guide to Methods and Applications*, M. A. Innis, D. H. Gelfand, J. J. Sninsky, T. J. White, Eds. (Academic Press, San Diego, 1990), p. 76]. The 19 NINAC p174 calmodulin binding fragments extended from the following amino acids: 955 to 1130, 996 to 1128, 1009 to 1146, 1012 to 1145, 1029 to 1141, 1032 to 1195, 1035 to 1193, 1038 to 1282, 1043 to 1182, 1045 to 1222, 1048 to 1211, 1051 to 1191, 1058 to 1197, 1062 to 1201, 1065 to 1198, 1067 to 1226, 1079 to 1219, 1085 to 1252, and 1087 to 1253.
20. J. A. Porter and C. Montell, *J. Cell Biol.* **122**, 601 (1993).
21. The NINAC proteins expressed in $P[ninaC^{KD}]$ and $P[ninaC^{MD}]$ were missing amino acids 17 to 284 and 331 to 1032, respectively. The p174 derivative expressed in $P[ninaC^{\Delta B}]$ was deleted for amino acids 1037 to 1253. The mutation in $P[ninaC^{\Delta B}]$ prevents the synthesis of p132. The sizes of the truncated forms of p174 expressed in $P[ninaC^{KD}]$, $P[ninaC^{MD}]$, and $P[ninaC^{\Delta B}]$ are 143, 93, and 145 kD, respectively. The transformants $P[ninaC^{KD}]$ and $P[ninaC^{MD}]$ were generated previously (*20*), and the *ninaC* mutation introduced into $P[ninaC^{\Delta B}]$ was generated by oligonucleotide-directed mutagenesis according to methods described in (*13*). Briefly, single-stranded DNA was generated from a BluescriptKS+ (Stratagene) construct containing a 2.9 kb Kpn I *ninaC* genomic fragment (9.0 to 11.9 map units) (*13*). This DNA was used to create a new Pst I site, by oligonucleotide-directed mutagenesis, at nucleotide 3902 to 3907 in the unique sequence encoding p174. The new Pst I site and the existing Pst I site at 3249 were used to delete the coding sequence from amino acids 1037 to 1253. This deleted version of the *ninaC* gene was subcloned into the *P*-element transformation vector pDM30 and introduced into $ninaC^{P235}$ and ry^{506} flies by *P*-element–mediated germline transformation [G. M. Rubin and A. C. Spradling, *Science* **218**, 348 (1982); A. C. Spradling and G. M. Rubin, *ibid.*, p. 341; D. Mismer and G. M. Rubin, *Genetics* **116**, 565 (1987)].
22. H. Swanljung-Collins and J. H. Collins, *J. Biol. Chem.* **267**, 3445 (1992).
23. E. Buchner, *J. Neurogenet.* **7**, 153 (1991).
24. B. T. Bloomquist *et al.*, *Cell* **54**, 723 (1988).
25. Z. Xia *et al.*, *Neuron* **6**, 431 (1991); Z. Xia *et al.*, *J. Neurochem.* **60**, 305 (1993).
26. C. W. Heizmann and K. Braun, *Trends Neurosci.* **15**, 259 (1992).
27. K. A. Alexander, B. M. Cimler, K. E. Meier, D. R. Storm, *J. Biol. Chem.* **262**, 6108 (1987); Y. Liu and D. R. Storm, *Trends Pharmacol.* **11**, 107 (1990).
28. J. R. Glenney Jr., A. Bretscher, K. Weber, *Proc. Natl. Acad. Sci. U.S.A.* **77**, 6458 (1980).
29. G. C. Johnston, J. A. Prendergast, R. A. Singer, *J. Cell Biol.* **113**, 539 (1991).
30. G.-H. Sun, Y. Ohya, Y. Anraku, *Protoplasma* **166**, 110 (1992); S. E. Brockerhoff and T. N. Davis, *J. Cell Biol.* **118**, 619 (1992).
31. Q. Zhu and M. Clarke, *J. Cell Biol.* **118**, 347 (1992).
32. Calmodulin overlays were performed as described by J. R. Glenney and P. Glenney [*Cell* **37**, 743 (1984)], except that the incubations were performed at room temperature with ^{125}I-labeled calmodulin (NEN) in the presence of 0.1 mM $CaCl_2$.
33. Calmodulin-agarose assays were performed as follows: Fly heads were homogenized at 4°C in a microfuge mortar and pestle (Kontes) in buffer A containing 10 mM imidazole (pH 7.35), 10% sucrose, 5 mM $MgCl_2$, 1 mM dithiothreitol, 160 mM KCl, PMSF (10 μg ml^{-1}), and leupeptin (1 μg ml^{-1}), and the homogenate was centrifuged at 100,000*g* for 30 min. Calmodulin-agarose (Sigma) was equilibrated in buffer A with several washs and then incubated for 30 min with the head extract supernatant. The extract-bead mixture was centrifuged at 3000*g* for 5 min, and the supernatant was combined with 1× volume of 2× SDS sample buffer and saved for gel analysis. The pellet was washed several times with buffer A plus 340 mM KCl and either 1 mM EGTA or 1 mM $CaCl_2$, and the bound proteins were eluted with SDS sample buffer (volume equal to 2× the supernatant volume). Samples were then fractionated by SDS-PAGE (6% gel).
34. The calmodulin antiserum was raised in rabbits as described by L. J. Van Eldik and D. M. Watterson [*J. Biol. Chem.* **256**, 4205 (1981)]. The antibodies were affinity-purified by their binding to calmodulin-Sepharose and eluted with 3 M sodium thiocyanate. To detect calmodulin from fly retinas, extracts from 25 retinas were prepared and fractionated on an SDS-PAGE (14% gel), transferred to PVDF membrane, and probed with the calmodulin antibody as described by D. Hulen and colleagues [*Cell. Motil. Cytol.* **18**, 113 (1991)], except that ^{125}I–protein A (NEN) was used instead of a secondary antibody.
35. In less than 10% of the $ninaC^{P235}$ samples, which were fixed only with paraformaldehyde, diffuse staining with the antibody to calmodulin was seen over the cell body and rhabdomeres, but when glutaraldehyde and paraformaldehyde were used for fixation, central matrix staining like that in Fig. 4C was seen consistently.
36. We thank D. W. Cleveland and D. J. Montell for helpful comments on this manuscript, J. Lee for technical assistance, and C. B. Klee for antibody to calmodulin. Supported by grant EY08117 from the National Eye Institute (C.M.), the National Science Foundation (Presidential Young Investigator Award to C.M.), and the American Cancer Society (Junior Faculty Research Award to C.M.).

28 May 1993; accepted 8 September 1993

Crystal Structure of Neocarzinostatin, an Antitumor Protein-Chromophore Complex

Kyoung-Hee Kim, Byoung-Mog Kwon, Andrew G. Myers,* Douglas C. Rees*

Structures of the protein-chromophore complex and the apoprotein form of neocarzinostatin were determined at 1.8 angstrom resolution. Neocarzinostatin is composed of a labile chromophore with DNA-cleaving activity and a stabilizing protein. The chromophore displays marked nonlinearity of the triple bonds and is bound noncovalently in a pocket formed by the two protein domains. The chromophore π-face interacts with the phenyl ring edges of Phe^{52} and Phe^{78}. The amino sugar and carbonate groups of the chromophore are solvent exposed, whereas the epoxide, acetylene groups, and carbon C-12, the site of nucleophilic thiol addition during chromophore activation, are unexposed. The position of the amino group of the chromophore carbohydrate relative to C-12 supports the idea that the amino group plays a role in thiol activation.

Neocarzinostatin (NCS) is a natural chromoprotein antibiotic isolated from *Streptomyces carzinostaticus* and is composed of a 113–amino acid protein component (apo-NCS) and a labile, nonprotein chromophore component (NCS-chrom) (*1*). A potent cytotoxic agent, NCS has undergone clinical evaluation for antitumor activity (*2*). In the presence of a thiol cofactor, NCS induces cleavage of single- and double-stranded DNA both in vivo and in vitro. The cleavage activity resides exclusively within the chromophore component (*1*), whose structure (*3*) (Fig. 1) was shown previously to include the epoxybicyclo[7.3.0]dodecadienediyne structural element. In vitro, NCS-chrom undergoes efficient thiol addition to form a highly reactive, carbon-centered biradical, which provides a potential molecular basis for the

Division of Chemistry and Chemical Engineering, California Institute of Technology, Pasadena, CA 91125.

*To whom correspondence should be addressed.